Salt Effects on Ionization Equilibria of Histidines in Myoglobin

Yung-Hsiang Kao,* Carolyn A. Fitch,† Shibani Bhattacharya,* Christopher J. Sarkisian,* Juliette T. J. Lecomte,* and Bertrand García-Moreno E.†

*Department of Chemistry, The Pennsylvania State University, University Park, Pennsylvania, 16802, and †Department of Biophysics, The Johns Hopkins University, Baltimore, Maryland 21218 USA

ABSTRACT The salt dependence of histidine pK_a values in sperm whale and horse myoglobin and in histidine-containing peptides was measured by ^{1}H-NMR spectroscopy. Structure-based pK_a calculations were performed with continuum methods to test their ability to capture the effects of solution conditions on pK_a values. The measured pK_a of most histidines, whether in the protein or in model compounds, increased by 0.3 pH units or more between 0.02 M and 1.5 M NaCl. In myoglobin two histidines (His^{48} and His^{36}) exhibited a shallower dependence than the average, and one (His^{113}) showed a steeper dependence. The ^{1}H-NMR data suggested that the salt dependence of histidine pK_a values in the protein was determined primarily by the preferential stabilization of the charged form of histidine with increasing salt concentrations rather than by screening of electrostatic interactions. The magnitude and salt dependence of interactions between ionizable groups were exaggerated in pK_a calculations with the finite-difference Poisson-Boltzmann method applied to a static structure, even when the protein interior was treated with arbitrarily high dielectric constants. Improvements in continuum methods for calculating salt effects on pK_a values will require explicit consideration of the salt dependence of model compound pK_a values used for reference in the calculations.

INTRODUCTION

Many properties of proteins, including their stability, solubility, catalytic activity, and ability to recognize and interact with other molecules, can be strongly dependent on the ionic properties of their milieu. Hydrogen ions and the ions of support electrolyte are the two main ionic components of the solutions in which physical properties of proteins are studied. The physical basis of pH effects is understood more completely than that of salt effects. The charged state of ionizable residues depends on the concentration of hydrogen ions; therefore, hydrogen ions can modulate equilibrium processes, such as conformational transitions, intermolecular associations, ligand binding events, etc., in which pK_a values of ionizable groups change (Wyman and Gill, 1990). Many experimental techniques for quantitating pH effects are available. For example, potentiometric methods make possible the direct measurement of the overall proton binding properties of proteins (García-Moreno et al., 1997), and NMR spectroscopy can probe the proton binding behavior of individual ionizable groups (Markley, 1975). Changes in the state of protonation of macromolecules during an equilibrium process can also be determined exactly, albeit indirectly, by analysis of the pH dependence of equilibrium constants with Wyman's classical linkage relationships (Chu et al., 1984; Wyman and Gill, 1990). An extensive theoretical framework based on classical electrostatic theory and statistical thermodynamics has been developed for structural interpretation of pH effects through pK_a calculations (Antosiewicz et al., 1994; Bashford et al., 1993; Matthew et al., 1985; Yang and Honig, 1994). In contrast, the physical origins of salt effects on proteins are poorly understood.

The problems with the interpretation of salt effects stem partly from the variety of modes with which proteins and ions can interact. Proteins are surrounded by an ionic double layer, the structure and properties of which are determined by the balance between disorganizing thermal forces and the organizing effects of electrostatic interactions and hydration at the protein-solvent interface. The properties of the double layer are influenced by the density of charged and polar groups on the surface of a protein. Therefore, salt and pH effects are thermodynamically coupled. Strong interactions between proteins and partially dehydrated, site-bound ions are not observed frequently. In general, the interactions between proteins and the ions of the double layer are weak and are not easily described in terms of concepts of mass action. One of the reasons for the continued poor understanding of these weak interactions is the lack of experimental methods for studying them directly and quantitatively. The effects of salts on equilibrium processes of proteins are usually investigated indirectly, by analysis of the salt dependence of equilibrium constants with linkage relationships (see Amiconi et al., 1981, for an example). Owing to the diversity of modes of interactions between ions and proteins, this approach is neither exact nor necessarily insightful, particularly concerning the structural meaning of the change in the number of thermodynamically bound ions.

Received for publication 31 March 2000 and in final form 2 June 2000.

Address reprint requests to Dr. Bertrand García-Moreno E., Department of Biophysics, The Johns Hopkins University, 3400 N. Charles St., Baltimore MD 21218. Tel.: 410-516-4497; Fax: 410-516-4118; E-mail: bertrand@jhu.edu; or to Juliette T. J. Lecomte, Chemistry Department, 152 Davey Laboratory, The Pennsylvania State University, University Park, PA 16802. Tel.: 814-863-1153; Fax: 814-863-8403; E-mail: jtl1@psu.edu.

Dr. Kao's present address is Analytical Chemistry, MS 62, Genentech, 1 DNA Way, South San Francisco, CA 94080.

0006-3495/00/09/1637/18 $2.00

The effects of salt on the stability of proteins are frequently interpreted in terms of screening of electrostatic interactions by the ionic strength. This concept was inherited from Linderstrøm-Lang. With characteristic genius, he applied the solution of the linearized Poisson-Boltzmann equation achieved by Debye and Hückel, less than a year after their original publication in 1923, to understand the ionization properties of proteins (Linderstrøm-Lang, 1924). The concept of ionic strength can account for general salt effects, those that are insensitive to the specific chemical nature of the salt. It cannot explain specific salt effects, which were appreciated early by enzymologists (Jencks, 1987) and in potentiometric proton titration studies of proteins (Tanford, 1961). Contemporary algorithms for structure-based pK_a calculations still depend solely on the Poisson-Boltzmann equation and on the concept of ionic strength to describe the effects of salts on the stability and energetics of proteins (Klapper et al., 1986; Matthew et al., 1985). Early attempts to account for specific salt effects in structure-based calculations treated some of the interactions between proteins and ions in terms of site-specific ion binding described by mass action (García-Moreno, 1994; Matthew et al., 1985). This approach was not pursued deeply for lack of useful experimental data with which to challenge and test calculations.

Many instances of salt-sensitive processes in proteins are difficult to explain with the simple concept of ionic strength as embodied in Poisson-Boltzmann electrostatics. The classic example is the regulation of functional properties of human hemoglobin. The oxygen- and proton-binding properties of this protein are highly sensitive to the specific nature of the anion (Amiconi et al., 1981), suggesting direct, chemical interactions between hemoglobin and anions. Recent examples include the effects of salts on the regulation of functional properties of other proteins (Dang and Di Cera, 1996) and on the interactions between proteins and nucleic acids (Kozlov and Lohman, 1998; O'Brien et al., 1998). Pronounced sensitivity to salt concentration has also been seen for the structure and stability of viral capsids (Fox et al., 1996) and other complex macromolecular assemblies. Refolding of acid-denatured proteins (Goto et al., 1990) and stabilization of mesophilic (Pace and Grimsley, 1988) and extremophilic proteins (Elcock and McCammon, 1998; Pieper et al., 1997) demonstrate further the thermodynamic importance of salt effects.

The understanding of the physical nature of interactions between proteins and ions continues to advance (Collins, 1997). However, at present there is no unifying theoretical framework based on simple physical principles capable of accounting quantitatively and structurally for all of the different types of salt effects that have been observed in proteins. To elucidate further the nature of interactions between proteins and ions and the structural basis of salt effects in equilibrium processes of proteins, the salt dependence of the pK_a of histidines in sperm whale (*Physeter catodon*) (Pc) and horse heart (*Equus caballus*) (Eq) myoglobin (Mb) was studied by ^{1}H-NMR spectroscopy. Several model peptides containing histidines were studied in parallel. Structure-based pK_a calculations were performed with continuum methods based on model-dependent or numerical solutions of the linearized form of the Poisson-Boltzmann equation. The aim of the calculations was to test the ability of the algorithms to describe the salt dependence of pK_a values of surface ionizable groups. The experimental data showed that, with a couple of remarkable and interesting exceptions, there is little difference between the effects of salt on ionization equilibria of histidines in Mb and those in model compounds. This suggests that the salt dependence of the ionization equilibria of surface histidines in proteins is not determined solely by screening of interactions between ionizable groups. The data underlined the need to revisit some of the notions that are commonly used to interpret structurally the effects of salts on the energetics of proteins.

MATERIALS AND METHODS

Protein and peptide samples

Horse Mb (type IV; Sigma, St. Louis, MO) and sperm whale Mb (Sigma) were used without further purification after extensive dialysis against distilled deionized water. The model compounds studied were Gly-His-Gly (Sigma); cyclo-Gly-His (Bachem, Torrance, CA); pyroGlu-His-Gly-NH_2 (pEHG-NH_2, Sigma); Lys-Ser-His-Pro-Glu (KSHPE) as a model for His[36]; and Phe-Lys-His-Leu-Lys (FKHLK) as a model for His[48]. The KSHPE and FKHLK peptides were synthesized by the solid-phase method and purified by reverse-phase high-performance chromatography at the Johns Hopkins Peptide Facility. The di- and tripeptides were used without further purification, except for Gly-His-Gly, which contained trace amounts of acetic acid. Before the experiments the pentapeptides and Gly-His-Gly were dialyzed extensively against distilled water.

NMR experiments

Proton NMR spectra were acquired in ^2H_2O on a Bruker AM-500 or a Bruker AMX2–500 spectrometer at 298 K, as previously described (Cocco et al., 1992). Experiments included one-dimensional pH titration as well as two-dimensional experiments to confirm the assignments throughout the pH and salt ranges. Nuclear Overhauser spectroscopy (NOESY) (Kumar et al., 1980) and total correlation spectroscopy (TOCSY) (Braunschweiler and Ernst, 1983; Cavanagh and Rance, 1992) data were collected in 90% ^1H_2O/10% ^2H_2O with and without added salt. For these experiments, a WATERGATE sequence with a 3-9-19 binomial pulse train was used to suppress the water signal (Piotto et al., 1992; Sklenár et al., 1993). A DIPSI (decoupling in the presence of scalar interactions)-2 (Shaka et al., 1988) or DIPSI-2rc (Cavanagh and Rance, 1992) pulse train was applied in the TOCSY experiments for isotropic mixing. The protein data were complemented with sets collected over a spectral width of 100,000 Hz, and with a water-eliminated Fourier transform (WEFT) (Inubushi and Becker, 1983) or driven-equilibrium Fourier transform (Hochmann and Kellerhals, 1980) sequence, to extract information from the paramagnetically shifted or relaxed signals (La Mar et al., 2000). WEFT-NOESY data were collected with a mixing time of 10 ms. Double-quantum-filtered correlated spectroscopy (DQF-COSY) (Rance et al., 1983) and CAMELSPIN (cross-relaxation appropriate for minimolecules emulated by locked spin) data (Bothner-By et al., 1984) were collected in ^2H_2O on one of the model peptides

(Lys-Ser-His-Pro-Glu, KSHPE) to confirm the configuration of the His-Pro peptide bond. Data processing was performed with the program FELIX (Molecular Simulations, San Diego, CA), using standard parameters (Cocco et al., 1992; Kao and Lecomte, 1993; Kao, 1994; Bhattacharya and Lecomte, 1997).

pH titrations

The procedure for the NMR pH titrations of metaquomyoglobin (metMbH_2O) was as reported previously (Cocco et al., 1992; Bhattacharya and Lecomte, 1997). The protein concentration ranged between 1 and 4 mM in ^2H_2O to remove amide resonances that interfered with the detection of the histidine Cϵ1H and Cδ2H resonances. Reproducibility trials indicated that the protein concentration did not alter the pK_a values. Typically, a protein solution at neutral pH was divided into two samples to be used in the high and low pH ranges. The pH of the solution was adjusted with 0.1 M NaO^{2}H or ^{2}HCl to record spectra every 0.2–0.3 pH units. Titrations were performed with various solution conditions: no added salt, 0.2 M, 0.5 M, and 1.5 M NaCl. KBr was also used in a subset of control titrations. In addition, a titration of horse heart Mb (Eq-Mb) was performed at near-saturated concentration of NaF (1.2–1.5 M). Under these conditions, the protein was in the metfluoride form, a high-spin species. The lowest pH that could be stably reached with metfluoride samples was near 6.2. This value was too high to obtain accurate pK_a values but was sufficient to notice trends.

For the experiments in different salt concentrations the acid and base solutions were prepared in the corresponding NaCl concentration. An approximate measurement of the salt concentration can be obtained by monitoring the chemical shift of the water line with respect to sodium 2,2-dimethyl-2-silapentane-5-sulfonate. With no added NaCl at 298 K, the water line occurs at 4.79 ppm. Over the 0–1.5 M NaCl concentration range, the shift varies linearly according to $\delta = (4.79 - [\mathrm{NaCl}] \times 0.1)$ ppm. This is in agreement with the number reported by Wishart and co-workers (1995).

A Beckman ϕ71 pH meter, equipped with an Ingold combination electrode (6030-1M), was used for pH measurements after two-point calibration with standard buffers (VWR Scientific, West Chester, PA) uncorrected for added salt. The pH of the protein solutions was determined before and after each NMR data collection. The readings were frequently identical; the largest discrepancies were below 0.05 unit; in cases of discrepancy, the reading after data collection was considered to be closest to the real value. The results were independent of the electrodes used. pH readings were not corrected for isotope effects because, at least in the case of histidines, these effects are balanced by a compensatory shift in the ionization equilibrium (Markley, 1975). To verify the approximation, titrations of cyclo-Gly-His were performed in 90% ^1H_2O/10% ^2H_2O and ^2H_2O in the absence of salt. The pK_a values were within experimental error of one another.

Titration data analysis

The chemical shift of resolved Cδ2H and Cϵ1H histidine resonances was used to prepare titration curves. The data were fitted to the sum of a modified Henderson-Hasselbalch equation (Eq. 1) and an unmodified Henderson-Hasselbalch equation (Eq. 2):

$$\delta_o = \delta_{His} + (\delta_{His^+} - \delta_{His}) \frac{10^{n(pK_a - pH)}}{1 + 10^{n(pK_a - pH)}}, \quad (1)$$

$$\delta_m = \Delta\delta_2 \frac{10^{(pH - pK_2)}}{1 + 10^{(pH - pK_2)}}. \quad (2)$$

Equation 1 represents the histidine titration, where δ_o is the chemical shift at any pH attributable to this titration alone, δ_{His} is the chemical shift of the neutral imidazole, δ_{His^+} is the chemical shift of the imidazolium ion, n is a Hill coefficient, and pK_a is the apparent ionization constant for the process. The latter four parameters are adjustable. Equation 2 contains two adjustable parameters (pK_2 and $\Delta\delta_2$) to take into account hemic acid dissociation (Brunori et al., 1968), by which the high-spin H_2O complex becomes a mixed-spin OH^- complex. The parameter δ_m represents the chemical shift change caused by the transition from the metaquo form to the methydroxy form of the protein at high pH. The observed chemical shift, δ, is the sum of δ_o and δ_m. In fitting the histidines that sense the alkaline transition, we fixed the parameter pK_2 to the value obtained from His^{48}, the residue most affected spectroscopically by the reaction. The assumptions implicit in the use of Eqs. 1 and 2 are that the protonation-deprotonation events are fast on the NMR time scale and that no additional titration event affects the observed curves. These assumptions were discussed in detail in temperature dependence experiments (Bhattacharya and Lecomte, 1997).

A single proton signal was chosen to represent the ionization constant of each residue. Whenever possible, the Cϵ1H signal was used in preference to the Cδ2H signal because of the larger chemical shift excursion experienced by the former. A variable degree of exchange broadening was observed for all signals at 11.4 T. This renders the interpretation of the Hill coefficient questionable (Sudmeier et al., 1980), and although it is found to vary, no precise significance was attributed to the change.

The methyl groups of Val^1 in sperm whale Mb (Pc-Mb) were followed to determine the N-terminus pK_a. Each methyl group gives a sharp doublet. The four chemical shifts were averaged, and the single value was used in the fit. The signals for Gly^1 in Eq-Mb could not be identified in the one-dimensional data sets.

His^{113} and His^{48} have low pK_a values, and their curves do not yield a precise δ_{His^+}. As described elsewhere (Bhattacharya and Lecomte, 1997), the number of adjustable parameters was reduced for these two residues by fixing the total chemical shift excursion to the value obtained at 288 K.

A normal titration curve is taken to yield a pK_a within $\pm$0.1 pH unit. The main sources of error are pH and salt concentration. To evaluate the effect of fluctuation of the latter throughout the titration, a simulation of the curve was performed in which the salt concentration (and therefore the pK_a) was varied monotonically on either side of pH 7, reaching 20 mM at the edge of the experimental pH range. This extreme but gradual change in conditions affected the most sensitive apparent pK_a value by less than 0.02 pH unit. The estimate suggests that the error introduced by the additions of acid and base is inconsequential compared to the other errors.

Measurement of overall proton titration curves

Proton titration curves were measured potentiometrically as described previously (García-Moreno et al., 1997). Measurements were performed in a thermostatted TTA 80 titration apparatus with a PHM 95 pH meter (Radiometer, Copenhagen, Denmark). The electrode chain consisted of separate glass (pH201; Radiometer) and calomel (Ref401; Radiometer) reference electrodes. All measurements and manipulations of protein solutions were carried out in CO_2-free solutions and environment. The isoionic point of Mb was determined by measuring the pH of the solution eluted from a strong, mixed-bed ion exchange column (Rexyn; Fisher Scientific, Pittsburgh, PA). The KCl concentration of samples was adjusted by the addition of a small volume of 3 M KCl stock.

The measurement of pH under conditions of high salt can give rise to experimental artifacts. Liquid junction potentials are introduced in the chain of electrodes, which can bias the measured pH. To demonstrate that this was not a source of artifactual pK_a shifts in 1.5 M salt, the pH of samples of water of different ionic strength was adjusted with acid between pH 5 and 9. The same amount of acid was needed regardless of ionic strength. This is consistent with the apparent activity of hydrogen ions in

the pH region of interest not being affected in a measurable manner by salts.

pK_a calculations

Structure-based pK_a calculations were performed with the structures for Mb from horse heart (Protein Data Bank accession code 1ymb) and from sperm whale skeletal muscle (Protein Data Bank accession code 4mbn). The existence of an ion paired His[36] in the structure of Mb in solution is suggested by the elevated pK_a measured by ^{1}H-NMR spectroscopy. The ion pair is not observed in the x-ray coordinates. It is apparently disrupted by intermolecular crystal contacts in this region of the protein. The ion pair is seen in the crystallographic structure of Mb from harbor seal skeletal muscle, where this set of intermolecular crystal contacts is absent (Scouloudi and Baker, 1978; Protein Data Bank accession code 1mbs). Therefore, the crystallographic structures 4mbn and 1ymb were modified by a single bond rotation of His[36] to establish arbitrarily an ion pair with 2.5 Å between Nδ1 of His[36] and Oϵ1 of Glu[38]. This adjustment is supported by the preference for the Nδ1H tautomer of the neutral ring observed by NMR spectroscopy (Bhattacharya et al., 1997; Bhattacharya and Lecomte, 1997).

Structure-based pK_a calculations were performed with two different methods. The finite-difference solution of the linearized Poisson-Boltzmann equation (FDPB) as implemented in the University of Houston Brownian dynamics (UHBD) software package was used for one set of calculations (Davies et al., 1991). The other set was performed with the solvent-accessibility-modified Tanford-Kirkwood method (SATK) developed by Gurd and co-workers (Matthew et al., 1985). Self-energies, or the sum of the Born and the background contributions, are not included in the calculation of pK_a values with the SATK algorithm. However, the lowest dielectric constant sampled in the calculations is 41 (the average of the dielectric constant of water and of the protein interior). For this reason the SATK method is thought to be useful for estimating pK_a values of surface ionizable groups (Matthew et al., 1985; Warshel et al., 1984). The structural and physical parameters used in the calculations with the SATK model are those already reported for calculations with Pc-Mb (García-Moreno et al., 1985). In previous applications of this algorithm the positive charge of the imidazole group was placed on one of the two possible nitrogen atoms, following criteria of ion pairing and solvent accessibility. In the present calculations the selection was made that maximized the agreement between the predicted and the experimental pK_a values under conditions of low ionic strength.

pK_a calculations with the FDPB method in the UHBD software suite were performed as described earlier (Antosiewicz et al., 1994). Polar hydrogen atoms were added to the crystallographic structures and energy minimized using CHARMm (version 25.2) (Molecular Simulations). Partial charges were taken from CHARMm (polar hydrogens only topology file, version 21), and atomic radii were taken from the OPLS parameter set (Jorgensen and Tirado-Rives, 1988). The titratable sites and intrinsic pK_a values used in the FDPB calculations were as follows: C terminus, 3.8; Asp Cγ, 4.0; Glu Cδ, 4.4; His Nδ1, 6.3; N terminus, 7.5; Tyr OH, 9.6; Lys Nζ, 10.4; and Arg Cζ, 12.0. The effects of the heme group on pK_a values were not included to avoid the complications related to handling the charge centers of the heme group. This approximation is supported by the earlier observation that removal of the heme in Mb has a limited effect on histidine pK_a values (Cocco et al., 1992). All calculations were performed at 298 K, the dimension of the Stern layer was 2.0 Å, the external dielectric constant was 80.0, the ion radius was 2.0 Å, and the dielectric constant in the interior of the protein was 20. Focusing was implemented as described by Antosiewicz et al. (1994), and the cluster method of Gilson (1993) was used to calculate the mean charge at every ionizable site. For both SATK and FDPB calculations, the pK_a values reported are the pH at the point of half-titration of the individual site isotherms.

Effects of site-specific anion binding on pK_a values

Calculations were also performed with a version of the SATK algorithm modified to account for specific salt effects that might arise from direct interactions between ionizable groups and partially desolvated site-bound ions (García-Moreno, 1994). The regions on the surface of Mb where the electrostatic potential ($\psi_{el,k}$) calculated with Eq. 3 exceeded $2kT$ were treated as putative sites of anion binding:

$$\psi_{el,k} = \sum_{j=1}^{n} \frac{560 Z_j (1 - SA_j)}{D_{eff} r_{kj}}. \quad (3)$$

In this empirical expression r_{kj} is the distance (Å) between point k on the surface of the protein and charge j. SA_j refers to the normalized solvent accessibility of charged atom j calculated with a probe radius of 1.4 Å, and Z_j is the pH-dependent fractional charge of titratable site j. D_{eff} is an effective dielectric constant obtained from the interaction energies calculated with the Tanford-Kirkwood formalism. Only contributions from ionizable groups to the surface electrostatic potential are included in the calculation of $\psi_{el,k}$.

The occupancy of anion-binding sites is computed as a function of salt concentration with a binding isotherm, using binding affinities ($K_{el,q}$) defined from electrostatic considerations:

$$K_{el,q} = K_{int} e^{-\Delta G_{el,q}/RT}. \quad (4)$$

Different values for the intrinsic anion binding constant (K_{int}) were explored. The binding energy $\Delta G_{el,q}$ represents the energy of interaction between the site-bound anion and the titratable sites in the protein. It was calculated with Eq. 5, using the electrostatic energies of pairwise interactions (W_{iq}) calculated with the Tanford-Kirkwood formalism:

$$\Delta G_{el,q} = \sum_{i=1}^{n} W_{iq} (1 - SA_{iq}) Z_i Z_q. \quad (5)$$

Reciprocal interactions between proton binding at the imidazole side chain and anion binding were handled explicitly with the Tanford-Roxby iterative approximation. The calculations assume that the binding constant of the anion is determined exclusively by charge-charge interactions (Eq. 5); the energetic penalty for desolvation of the anion concomitant with binding is not included in the calculation of ion binding energetics. This approximation is probably valid for the case of anions, which are only solvated weakly and which retain considerable contact with bulk water when bound to the surfaces of proteins. The effects of site-specific Cl^- binding on pK_a values were not studied with the FDPB method because of the problems inherent to the explicit treatment of hydration in these calculations.

RESULTS

Histidine assignments in Mb ^{1}H-NMR spectra

Spectral assignments for histidines in Pc-Mb and Eq-Mb in the absence of salt were as reported previously (Cocco et al., 1992; Bhattacharya et al., 1997; Bhattacharya and Lecomte, 1997). His[64], His[93], and His[97] are close to the heme and are not detected in the metMbH_2O complex. However, an estimate of the pK_a value can be obtained indirectly for His[97]. This histidine is in van der Waals contact with the heme pyrrole D, which bears the 5-methyl group. By monitoring the chemical shift of the 5-methyl resonance in metcyano

Mb (a low-spin complex), Krishnamoorthy and La Mar (1984) determined the pK_a of His^{97} to be 5.3. In metMbH$_2$O, the pH response of the heme 5-methyl group yielded a pK_a of 5.1 in the absence of salt. Although the determination of a pK_a for His^{97} is useful for comparison with potentiometric data, the measurements in the presence of salt were not sufficiently reliable and His^{97} was not considered further.

Effect of salt on histidine pK_a values in Mb

^{1}H-NMR pH titrations of Pc-Mb and Eq-Mb were carried out at several NaCl concentrations. A small number of control titrations were also performed with KBr instead of NaCl; these yielded the same results within experimental error. The lowest salt concentration corresponds to extensively dialyzed samples, which were expected to contain up to 0.02 M salt at pH extremes. Other salt concentrations were obtained by preparing the protein samples in solutions containing 0.2, 0.5, and 1.5 M NaCl. Typical chemical-shift-versus-pH data were similar to those reported elsewhere (Cocco et al., 1992; Bhattacharya and Lecomte, 1997) and were fitted to the Henderson-Hasselbalch equations (Eqs. 1 and 2) to obtain individual titration parameters. These were then used to calculate the fractional charge (Z) carried by each imidazole ring as a function of pH. Fig. 1 contains the resulting Z plots for four representative histidines in Pc-Mb: His^{36} (Fig. 1 *A*), His^{48} (Fig. 1 *B*), His^{81} (Fig. 1 *C*), and His^{113} (Fig. 1 *D*).

His^{81} yields complete titration curves, whereas His^{36}, His^{48}, and His^{113} do not. Their pK_a values are such that one of the limiting chemical shift values (basic end point in the case of position 36, acidic end point in the cases of positions 48 and 113) cannot be measured directly. Furthermore, at 500 MHz in the absence of buffer, practically all histidines, but particularly His^{36} and His^{113}, broaden through the transition. Despite these known difficulties, the pH responses were sufficiently defined by the experimental data in the presence of salt; pK_a values could be extracted and trends recognized. Thus added NaCl had a detectable effect on the pK_a of His^{113}, and this effect was significantly larger than the effect on His^{36} and His^{48}. Similar data were analyzed for other histidines in Eq-Mb and Pc-Mb. All values are listed in Tables 1 (Pc) and 2 (Eq) and pK_a values are plotted as a function of log [NaCl] in Figs. 2 and 3. For purposes of discussion, it is useful to group the histidines into four classes, as described below.

Class 1 histidines: 12, 48, 81, 116, and 119

Despite differences in their accessibility to solvent, pK_a values, and distribution of charged and polar residues in

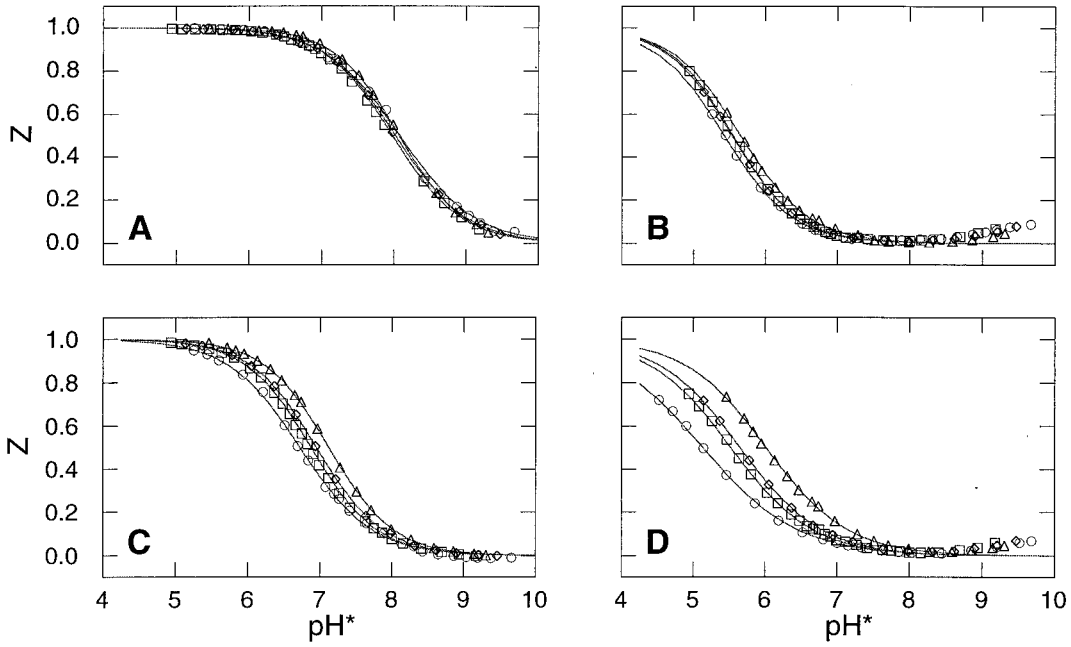

FIGURE 1 Fractional charge (Z) of selected histidines in Pc-Mb versus pH* (pH uncorrected for isotope effects) at NaCl concentrations of 0.02 M (○), 0.20 M (□), 0.50 M (◇), and 1.50 M (△). Data are shown for (*A*) His^{36} (class 2 residue; see classification in text); (*B*) His^{48} (class 1); (*C*) His^{81} (class 1); and (*D*) His^{113} (class 3). The raw experimental data were fitted simultaneously to Henderson-Hasselbalch equations 1 (histidine ionization) and 2 (hemic acid dissociation). Histidine pK_a values (listed in Table 1), Hill coefficients, and limiting chemical shifts obtained as fitted parameters for Eq. 1 were used to calculate the Z curves shown in the figure. Deviations from the Z curves at high pH are attributed to the formation of methydroxy Mb in the hemic acid dissociation represented by Eq. 2 and are particularly pronounced for His^{48} and His^{113} (Cocco et al., 1992).

TABLE 1 Histidine pK_a values in sperm whale Mb as a function of NaCl concentration

		0.02 M*	0.2 M†	0.2 M KBr‡	0.5 M‡	1.5 M‡
His^{12}	Cε1H	6.38 (0.01)	6.49 (<0.01)	6.57 (<0.01)	6.52 (<0.01)	6.68 (<0.01)
His^{36}	Cε1H	8.08 (0.01)	7.98 (<0.01)	7.97 (0.02)	8.02 (<0.01)	8.07 (<0.01)
His^{48}	Cε1H	5.42 (0.02)	5.55 (<0.01)	5.61 (0.02)	5.52 (<0.01)	5.65 (<0.01)
His^{81}	Cε1H	6.72 (0.01)	6.88 (0.01)	6.97 (0.01)	6.95 (<0.01)	7.12 (<0.01)
His^{113}	Cδ2H	5.13 (0.02)	5.51 (0.02)	5.61 (0.03)	5.65 (0.02)	6.01 (0.01)
His^{116}	Cε1H	6.59 (0.02)	6.70 (0.01)	6.78 (0.01)	6.74 (0.01)	6.89 (0.01)
His^{119}	Cδ2H	6.16 (0.03)	6.26 (0.01)	6.37 (0.01)	6.33 (0.01)	6.69 (0.02)
	His^{-24}§	6.03 (0.03)	6.19 (0.01)	6.30 (0.01)	6.27 (0.02)	6.64 (0.02)
Val^{1}	CγH_3's¶	7.47 (0.07)	7.52 (0.05)		7.63 (0.06)	7.67 (0.04)

All values were obtained at 298 K.

*Average of two independent measurements obtained on extensively dialyzed samples. The NaCl concentration is an estimate. Uncertainties shown in parentheses are (average) standard deviations from individual fits.

†Average of two independent measurements.

‡Single measurement.

§His^{24}, a class 4 histidine, remains in the neutral state, even at low pH. However, the Cε1H of His^{24} senses the titration of His^{119} (Cocco et al., 1992). These values for His^{119} were determined using His^{24} Cε1H.

¶Fit to the average chemical shift of four resonances from the γ methyl groups.

their vicinity, these histidines behaved similarly with respect to salt addition. They exhibited a modest rise in pK_a up to NaCl concentrations of 1.5 M. The increase was independent of the absolute value of the pK_a, and the values in adjacent salt concentrations were within experimental error of each other. In addition, for most histidines the salt dependence of the pK_a between salt concentrations of 0.02 M and 0.50 M was smaller than the increase between 0.50 and 1.50 M NaCl. His^{119}, when monitored directly or through His^{24}, displayed an exaggerated response at the highest salt concentration, whereas His^{48} had the shallowest salt dependence in this class, with nearly indistinguishable values at the extremes in NaCl concentration.

Class 2 histidines: 36

His^{36} showed an elevated pK_a insensitive to salt between 0.02 M and 1.5 M NaCl.

Class 3 histidines: 113

His^{113} has a depressed pK_a under conditions of low NaCl concentration. Its pK_a increased by 0.4 units between 0.02 and 0.20 M NaCl, and by 0.35 units between 0.2 and 1.5 M NaCl (Tables 1 and 2). At 1.5 M NaCl, the pK_a had not yet reached the value of a solvent-exposed histidine, and no evidence of leveling off was observed.

Class 4 histidines: 24, 64, 82, 93, and 97

Class 4 contains the remaining histidines. Among these, only His^{24} and His^{82} can be monitored directly in the metMbH_2O form. These histidines are mostly buried and remain predominantly in the neutral state down to the lowest accessible pH values with the soluble native state. The onset of the titration curve displayed by His^{82} moved to higher pH values as the salt concentration was increased. In

TABLE 2 Histidine pK_a values in horse Mb as a function of NaCl concentration

		0.02 M*	0.2 M†	0.2 M‡	0.5 M†	1.5 M§
His^{36}	Cε1H	7.67 (0.01)	7.80 (0.02)	7.78	7.73 (0.02)	7.83 (0.02)
His^{48}	Cε1H	5.42 (0.02)	5.62 (0.01)	5.57	5.68 (0.01)	5.69 (0.03)
His^{81}	Cε1H	6.65 (0.01)	6.94 (0.01)	6.89	6.92 (<0.01)	7.04 (0.01)
His^{113}	Cδ2H	5.51 (0.02)	5.87 (0.02)	5.83	6.01 (0.02)	6.15 (0.02)
His^{116}	Cε1H	6.66 (0.02)	6.79 (0.01)	6.78	6.78 (0.02)	6.85 (0.01)
His^{119}	Cδ2H	6.38 (0.02)	6.56 (0.01)	6.54	6.54 (0.01)	6.70 (0.01)
	His^{24}¶	6.28 (0.02)	6.50 (0.02)		6.52 (0.02)	6.68 (0.02)

All values were obtained at 298 K.

*Average of three independent measurements obtained on extensively dialyzed samples. The NaCl concentration is an estimate. Uncertainties shown in parentheses are (average) standard deviations from individual fits.

†Average of two independent measurements.

‡Calculated with the parameters reported in the variable temperature study of Bhattacharya and Lecomte (1997).

§Single measurement.

¶Value for His^{119} as sensed by His^{24} Cε1H (see note § of Table 1).

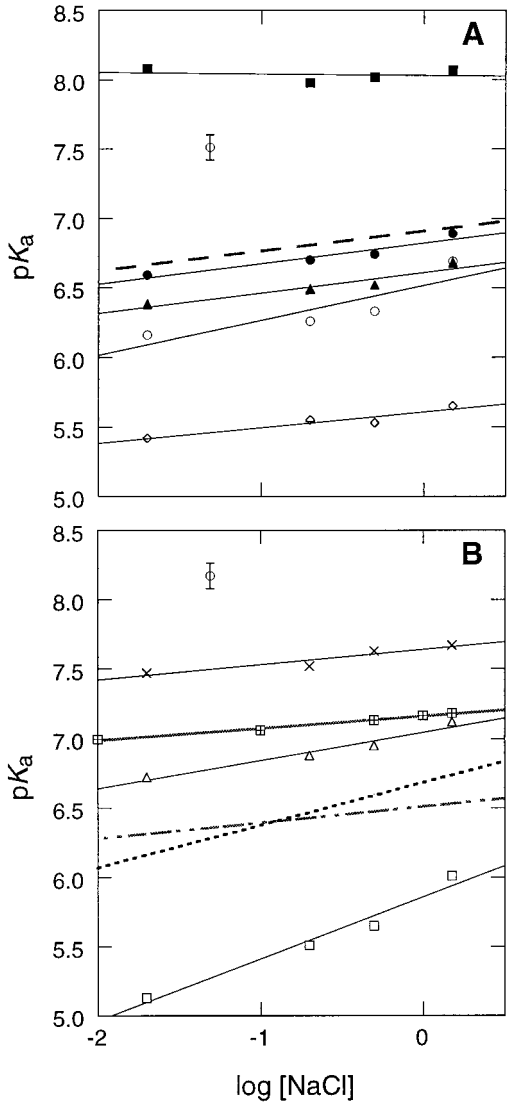

FIGURE 2 Salt dependence of pK_a values of histidines in Pc-Mb measured by ^{1}H-NMR spectroscopy. The data are plotted over two panels for clarity. The artificial data point at the top of each panel indicates the size of the experimental error. (*A*) His^{36} (■), His^{116} (●), His^{12} (▲), His^{119} (○), and His^{48} (◇). A straight line has been fitted to the points only to guide the eye. The dashed line (– – –) represents the fit to the data for the histidine in GHG. (*B*) N-terminus amino group. (×), His^{81} (△) and His^{113} (□). A straight line has been fitted to the points only to guide the eye. Lines are also included for the histidines in pEHG-NH$_2$ (– – ·· – –), and FKHLK (·····) peptides for comparison. (⊞), effects of salts on the pK_a of a blocked histidine, calculated relative to a pK_a of 7.0 at 0.02 M NaCl from solvation energies obtained with FDPB.

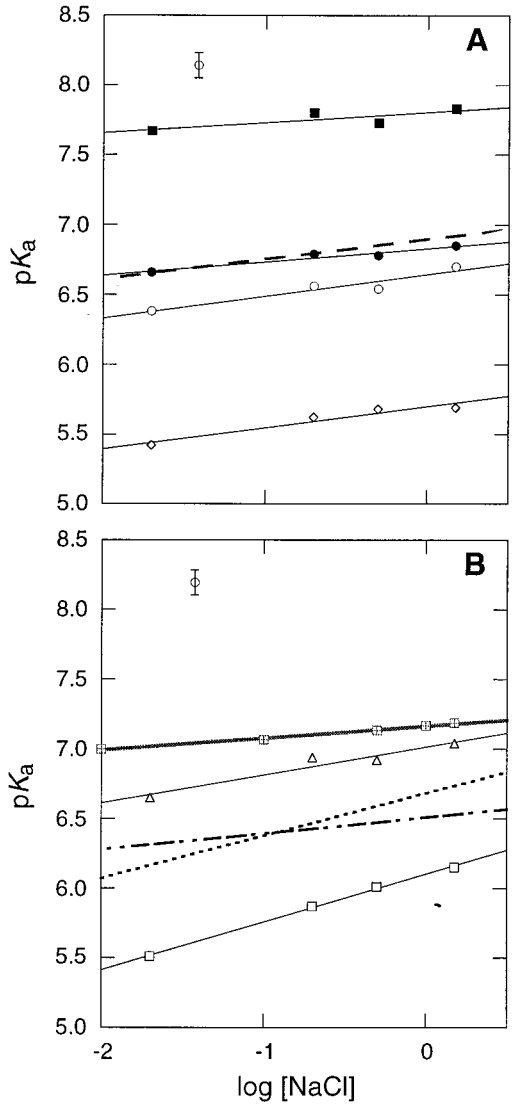

FIGURE 3 Salt dependence of pK_a values of histidines in Eq-Mb measured by ^{1}H-NMR spectroscopy. The data are plotted over two panels for clarity. The artificial data point at the top of each panel indicates the size of the experimental error. (*A*) His^{36} (■), His^{116} (●), His^{119} (○), and His^{48} (◇). A straight line has been fitted to the points only to guide the eye. The dashed line (– – –) represents the fit to the data for the histidine in GHG. (*B*) His^{81} (△) and His^{113} (□). A straight line has been fitted to the points only to guide the eye. Lines are also included for the histidines in pEHG-NH$_2$ (— ·· —) and FKHLK (·····) peptides for comparison. (⊞), effects of salts on the pK_a of a blocked histidine, calculated relative to a pK_a of 7.0 at 0.02 M NaCl from solvation energies obtained with FDPB.

the absence of a complete curve, it was not possible to determine whether this was a manifestation of a large pK_a alteration. On the other hand, even at the highest salt concentration, His^{24} did not exhibit any sign of its own titration. The ionization of several histidines in class 4 is linked to conformational changes (Barrick et al., 1994), and these histidines will not be discussed further.

Effect of salt on histidine pK_a values in model compounds

Measuring accurate pK_a values in the presence of support electrolyte of concentrations higher than 50 mM can be complicated by the effects of ions on the liquid junction potentials of pH electrodes and on the activity of hydrogen ions. In addition, the chemical shift parameter is sensitive

not only to protonation state but also to conformational disruptions and other nearby protonation events. To assess systematic errors and to establish a reference behavior, the following model compounds were subjected to the same titration procedure as applied to the proteins: imidazole, the linear unprotected Gly-His-Gly, the cyclic dipeptide cyclo-Gly-His, the blocked tripeptide pyroGlu-His-Gly-NH_2, and two pentapeptides corresponding to the amino acid sequences surrounding His^{36} (KSHPE) and His^{48} (FKHLK). Table 3 and Fig. 4 contain the results of NMR titrations carried out on these small peptides. In the case of KSHPE, two sets of signals were observed for the central histidine, yielding two distinct pK_a values. Two-dimensional experiments revealed that the peptide was present in a mixture of slowly exchanging *cis* (KSHPEc) and *trans* (KSHPEt) forms of the His-Pro peptide bond. No evidence for the *cis* conformer was detected in the protein data.

Under conditions of low salt concentration the pK_a values clustered near 6.6 or 6.2. With the addition of NaCl, the values increased in a fashion reminiscent of class 1 histidines, with the exception of the histidine in FKHLK, the pK_a of which increased by 0.6 pH units between 0.02 M and 1.5 M NaCl. Its steep dependence on salt concentration was attributed to the screening of the two positively charged lysines.

The effects of salt on the proton titration curves of imidazole and of the cyclo-Gly-His peptide were measured potentiometrically (data not shown) and found to be consistent with the effects evidenced by NMR spectroscopy. The potentiometric measurements also showed that the pK_a of imidazole was shifted by 0.2 pH unit between low NaCl and 1.5 M NaCl, and no further increase in pK_a was detected at higher salt concentrations.

Fig. 4 contains the results of two pK_a calculations describing the effects of salt concentration on the ionization equilibrium of a histidine. One of them (Fig. 4, *filled circles*) used Eq. 6, derived by Davies (1938). This equation estimates the ionic strength dependence of the pK_a:

$$pK_a(I) = pK_a(0) + \left\{\frac{0.5I^{1/2}}{1 + I^{1/2}} - 0.10I\right\}, \qquad (6)$$

TABLE 3 Histidine pK_a values in model peptides as a function of NaCl concentration

	0.02 M†	0.2 M	0.5 M	1.5 M
GHG	6.68	6.78	6.85	6.96
pEHG-NH_2	6.30	6.46	6.47	6.52
cGH	6.18	6.28	6.43	6.48
FKHLK	6.16		6.60	6.73
KSHPE-*trans*	6.69		6.78	6.83
KSHPE-*cis*	6.23		6.38	6.48

Average of Cδ2H and Cε1H values, at 298 K.
†Obtained on samples against water without any added salt. The NaCl concentration is an estimate. Standard deviations of the fit are 0.02 or better.

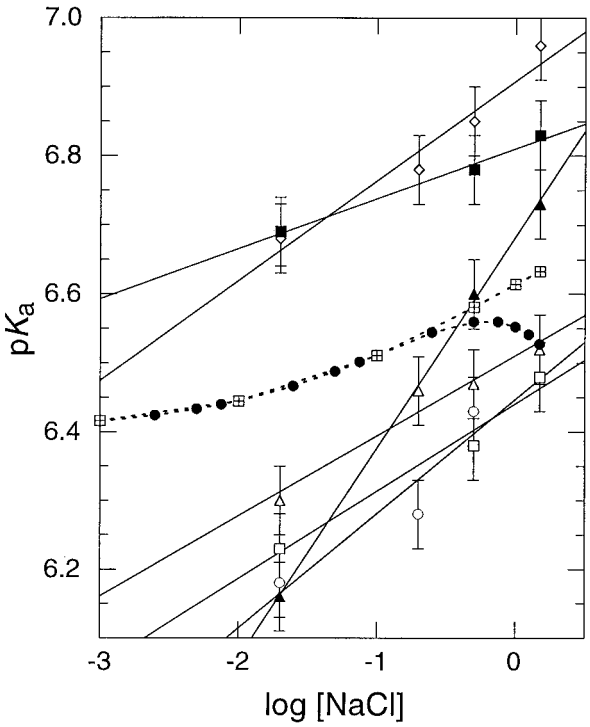

FIGURE 4 pK_a values of histidine residues in model peptides measured by ^{1}H-NMR spectroscopy. Lines represent fits to the data for GHG (◇), pEHG-NH_2 (△), cyclo-GH (○), FKHLK (▲), the major component of KSHPE (■, KSHPE*t*), and the minor component of KSHPE (□, KSHPE*c*). Dotted lines join the pK_a values calculated, relative to a pK_a of 6.4 at 0 M NaCl, with Eq. 6 (●) and from solvation energies of a blocked histidine calculated with FDPB (⊞).

where p$K_a(I)$ denotes the value at ionic strength I in M. Also shown in Fig. 4 is the salt dependence of the pK_a value of a blocked histidine estimated from solvation energies calculated with FDPB (*crossed squares*). These solvation energies were calculated as differences of self-energies of the charged and neutral forms of the histidine, in vacuum and in solution. Although this calculation is also based on the linearized Poisson-Boltzmann equation, a limiting law not valid at high salt concentrations, the magnitude and direction of the shift in pK_a were reasonable, even at 1.5 M NaCl.

Agreement between macroscopic and microscopic proton titration behavior

The differences between histidine pK_a values measured by NMR methods under conditions of low and high NaCl concentration were small on average (Tables 1 and 2). However, given the large number of titrating histidine residues in Mb, the summed effect on the total charge of the protein is significant. Potentiometric experiments were therefore performed to corroborate the NMR results. The data in Fig. 5 describe the pH dependence of the charge of

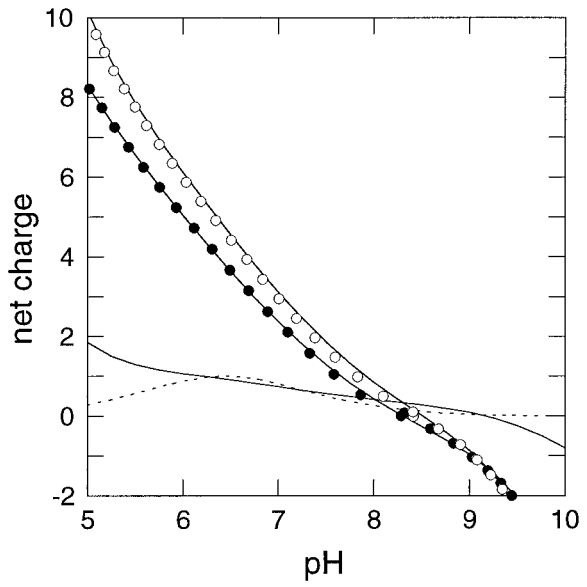

FIGURE 5 Proton titration curve of Pc-Mb measured potentiometrically in 0.1 M KCl (●) and in 1.0 M KCl (○). Lines through the experimental data points represent fits with fifth-order polynomials. The solid line in the bottom section of the figure represents the difference between the two proton binding curves. The dotted line represents the difference in the proton titration behavior in 0.2 M and 1.5 M NaCl, calculated with the pK_a values of histidines and the amino terminus listed in Table 1.

Pc-Mb in 0.1 M and 1.0 M KCl. KCl was used instead of NaCl to minimize the sodium error of the electrode at high ionic strengths and to prevent the introduction of additional liquid junction potentials in the chain of electrodes. The difference between the charged states of Mb in these two salt concentrations reflects the net effect of salt on the pK_a values of all ionizable residues. The difference titration curve in Fig. 5 shows that near neutral pH the shift in pK_a values at high salt concentration resulted in the uptake of an entire proton relative to low salt conditions. The net difference in the charge of the protein between 0.2 M and 1.5 M NaCl was also calculated with the pK_a values measured by NMR spectroscopy (Table 1). The difference titration curve predicted from the pK_a values in Table 1 was indistinguishable from the curve measured potentiometrically in the neutral range of pH. The disagreement between experimental and calculated difference titration curves at pH values below 6 was likely to reflect the contributions of other titrating groups, including some of the class 4 histidines.

The agreement between the macroscopic titration properties and the sum of the titration curves of the individual histidine residues is significant. It shows that the NMR method, despite potential complications due to the extreme sensitivity of the chemical shift variable to solution conditions, is reliable for the evaluation of differences in pK_a values measured at low and high salt concentrations.

Effects of NaCl and pH on the structure of Mb

Two-dimensional ^{1}H-NMR data were collected to probe protein structural integrity as a function of NaCl concentration and pH. At pH 5.7, extensive comparison of solution data with solid-state structure prediction reveals no major discrepancies (Kao and Lecomte, 1993; Kao, 1994). As the pH was raised, NOEs characteristic of each histidine could be detected. For nontitrating residues and for residues remote from titrating groups, the chemical shift provides an indicator of structural perturbation. The location of assigned cross-peaks was therefore monitored as a function of salt concentration. When chemical shifts at one NaCl concentration were compared to those at another NaCl concentration, small differences were observed throughout the structure, but only a few signals moved by more than two standard deviations from the average deviation. The perturbed regions were near lysine residues (Kao, 1994). Typical NOEs were maintained up to 1.5 M NaCl between His^{24} and Arg^{118}, His^{113} and Arg^{31}, His^{36} and Phe^{106}, and His^{82} and Leu^{86}. The conclusion from the data sets collected at various salt concentrations and pH values was that structural rearrangements were apparently minor, even for charged groups.

Comparison between experimental and calculated salt effects on histidine pK_a values

The pK_a values calculated for Pc-Mb with the SATK method are listed in Table 4, and the comparison between calculated and measured pK_a values for class 1 histidines is presented in Fig. 6 *A*. Results for Eq-Mb are similar and are not shown. To facilitate comparison of the salt dependence of measured and calculated pK_a values, the calculated values were translated along the ordinate to force coincidence with the experimental data at 0.02 M. At salt concentrations below 25 mM, the pK_a values calculated with the SATK method in general match the experimentally observed values. This reflects partly the arbitrary manner in which the charge-bearing nitrogen of the imidazole groups was selected. The agreement is a consequence of the use of high effective dielectric constants in the SATK algorithm to compute the energies of interaction between surface ionizable sites. It has been recognized previously that methods that use high effective dielectric constants can capture realistic energetics of ionization of surface groups (Warshel et al., 1984).

In the case of His^{48} the agreement between the measured and the calculated pK_a at low NaCl concentration was not satisfactory. The failure of the SATK method to capture correctly the depressed pK_a of this residue suggested that it is determined by loss of hydration upon burial rather than by interactions with other ionizable groups. This is supported by temperature dependence data (Bhattacharya and Lecomte, 1997).

TABLE 4 Histidine pK_a values in sperm whale Mb, calculated with structure-based methods

	SATK				FDPB			
	0.02 M	1.5 M	Δcalc*	Δexpt†	0.01 M	1.5 M	Δcalc*	Δexpt†
His^{12}	6.38	6.50	0.12	0.0	6.01	6.09	0.08	−0.37
His^{24}	—	—	—	—	4.97	5.29	0.32	—
His^{36}	7.87	7.60	−0.27	−0.21	7.23	7.17	−0.06	−0.85
His^{48}	5.98	6.01	0.03	0.56	5.40	5.70	0.30	−0.02
His^{81}	6.76	6.66	−0.10	0.04	6.06	6.37	0.31	−0.66
His^{113}	5.14	5.62	0.48‡	0.01	4.49	5.15	0.66	−0.64
His^{116}	6.57	6.59	0.02	−0.02	6.23	6.23	0.00	−0.36
His^{119}	6.08	6.39	0.31	−0.08	4.30	4.86	0.56	−1.86

*Δcalc = pK_a (1.5 M) − pK_a (0.01 M).
†Δexpt = pK_a (0.01 M or 0.02 M; calculated) − pK_a (0.02 M; experimental).
‡Calculated without site-bound Cl^-.

In calculations with the SATK method salts can only perturb pK_a values by screening Coulombic interactions between ionizable sites. Thus in the case of histidines with a pK_a higher than the intrinsic values at low salt concentration (His^{36}, His^{81}), the effect of increasing salt is to decrease the pK_a. The converse is true for histidines with depressed pK_a values (His^{12}, His^{119}, His^{113}). In Fig. 6 *A* it can be seen that at high salt concentrations the calculated pK_a values of all class 1 histidines tend toward the intrinsic pK_a of 6.6 or 6.0. This trend differs from what was observed experimentally. The lack of agreement between the salt dependence of measured pK_a values and the values estimated with SATK calculations underscores the problems that arise from the lack of a self-energy term in those calculations.

The pK_a values estimated for class 1 histidines with the FDPB method are listed in Table 4 and shown in Fig. 6 *B*. The calculated pK_a values in Fig. 6 *B* were also translated along the ordinate to force coincidence with experimental pK_a values at 0.02 M. Calculations with a protein dielectric constant of 4 predict grossly incorrect ionization energetics. An arbitrary value of 20 was used instead to improve the agreement between calculated and measured pK_a values (Antosiewicz et al., 1994, 1996). With the exception of His^{119}, this led to an acceptable reproduction of experimental values. However, the pK_a values calculated with FDPB were systematically lower than those measured by NMR spectroscopy and not as close to the experimental numbers as those calculated with the SATK method. Even when the protein dielectric constant is 20, the calculations with the FDPB method overestimate the contribution of long-range interactions to the electrostatic energies. At pH values near the pK_a of histidines the net charge of Mb is positive; thus the pK_a values are artificially depressed when they are obtained from the FDPB calculations.

The FDPB pK_a values contained the assumption that the Nδ1 atom is the charge-bearing atom of the protonated form of histidine. Calculations where the Nϵ2 atom was selected instead yielded similar pK_a values for His^{12}, His^{36}, His^{48}, His^{81}, and His^{116}. In the case of His^{24} the calculated pK_a was much lower when the Nϵ2 atom was selected as the charge-bearing atom. The pK_a of His^{119} also depended somewhat on the tautomer assignment. Furthermore, the pK_a values of His^{113} and His^{119} were closer to the experimental values when the Nϵ2 atom was arbitrarily selected as the charge-bearing atom. At salt concentrations above 10 mM the salt dependence of pK_a values calculated with FDPB was independent of how the charge-bearing atom was selected, even in the case of His^{113} and His^{119}.

Overall, there was apparent agreement between the salt dependence of FDPB pK_a values and the observed values at salt concentrations 0.10 M and lower. At higher salt concentrations the estimated pK_a values were lower than the measured values. In the case of His^{81} and His^{48}, the FDPB calculations simulated the effects of salt better than the SATK calculations. Although there were cases, such as His^{119}, in which the SATK calculations appeared to describe the observed salt dependence of a pK_a better than FDPB calculations, the trend showed that FDPB calculations provided a physically more realistic quantitative estimation of the effects of salts on pK_a values.

Salt dependence of the pK_a of an ion-paired histidine

The comparison of pK_a values for His^{36} as measured by NMR methods and calculated with SATK and FDPB methods is presented in Fig. 7. The calculated curves in this figure were translated along the ordinate to cross the experimental value at 0.02 M NaCl. Also included in Fig. 7 (*dashed line*) is the effect of ionic strength on the Gibbs energy of interaction between a pair of charges embedded in an aqueous medium, calculated with a simple Coulombic potential and a Debye-Hückel parameter to account for screening by the ionic strength:

$$\Delta pK_a = \frac{332 Z_i Z_j}{2.303 RT r_{ij} D_{H_2O} e^{\kappa r_{ij}}}. \quad (7)$$

In this equation Z_i and Z_j refer to the valence of the charges in the pair, κ is the Debye-Hückel parameter, proportional

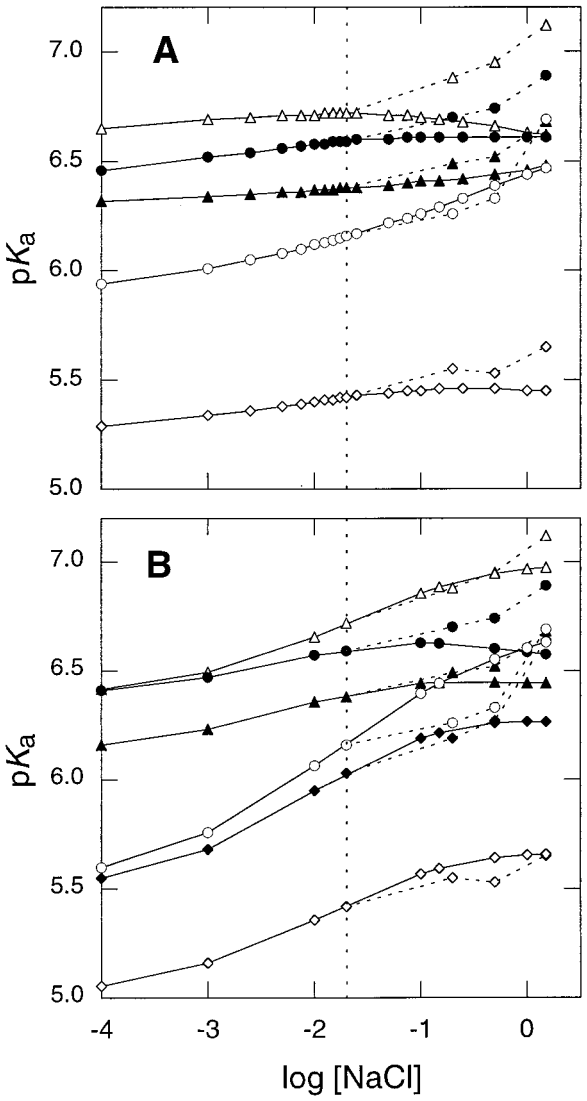

FIGURE 6 Comparison between calculated and observed salt dependence of pK_a values of histidines in Pc-Mb: His^{12} (▲), His^{24} (♦), His^{48} (◇), His^{81} (△), His^{116} (●), and His^{119} (○). The lines joining the experimental data points (- - - -) and the calculated values (——) were drawn to guide the eye. (*A*) pK_a values calculated with the SATK algorithm. (*B*) pK_a values calculated with FDPB, using $D_{prot} = 20$. The calculated pK_a curve of each histidine in *A* and *B* has been individually shifted along the ordinate to force passage through the experimental pK_a at 0.02 M NaCl. This concentration is marked by a vertical dotted line.

to the square root of $I/D_{H_2O} \times T$, where I is the ionic strength in M, D_{H_2O} is the dielectric constant of water, and T is the absolute temperature in K.

Equation 7 expresses the notion that increasing ionic strength weakens ion pairs. It predicts that the energy of interaction between a pair of unit charges separated by 2.5 Å is screened effectively between 1×10^{-4} M and 0.2 M ionic strength. In contrast, the experimental pK_a of His^{36} was insensitive to NaCl over the range 0.02–1.5 M. This was captured correctly in the SATK calculations up to 0.5 M NaCl and in the FDPB calculations up to 1.5 M NaCl.

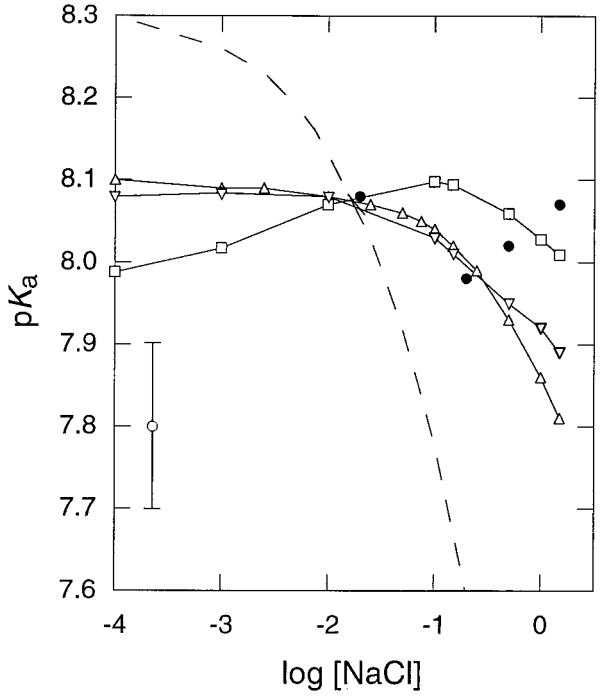

FIGURE 7 Comparison between calculated and observed salt dependence of the pK_a of His^{36} in Pc-Mb. (●), the experimental data. Solid lines join the pK_a values calculated by SATK (△), and by FDPB, using $D_{prot} = 20$ (□) or $D_{prot} = 4$ (▽). A thin dashed line describes the salt dependence of the interaction energy between an ion pair in solution separated by 2.5 Å, as predicted with Eq. 7, using $D_{H_2O} = 50$. All calculated pK_a values have been shifted along the ordinate to force coincidence with the experimental data point at 0.02 M NaCl as in Fig. 6. Compared to Fig. 6, the vertical scale has been changed. A measure of the experimental error is indicated by an artificial data point at the bottom of the panel.

Salt dependence of the pK_a of a histidine in contact with a basic group

In the crystal structures of Pc-Mb the average distance between all of the nitrogen atoms of His^{113} and Arg^{31} is 3.8 Å. The depressed pK_a of His^{113} presumably reflects the strongly repulsive interactions between these two groups. Relative to an intrinsic pK_a of 6.6, the low pK_a of His^{113} represents 8.2 kJ/mol of destabilizing interaction. Increasing concentrations of salt are singularly effective in attenuating this repulsive interaction. The comparison between the experimentally determined pK_a values of His^{113} and the values predicted by SATK and by FDPB calculations is presented in Fig. 8 A. The finite difference calculation reproduced the absolute value and the salt dependence of the pK_a of His^{113} well. The pK_a calculated with SATK also agreed well with the experimental value at 0.02 M NaCl, but the predicted dependence on increasing salt concentrations was not as steep as that observed by NMR spectroscopy.

Fig. 8 also includes data from an SATK calculation in which the occupancy of an anion binding site defined by His^{113} and Arg^{31} and the coupling between the protonation

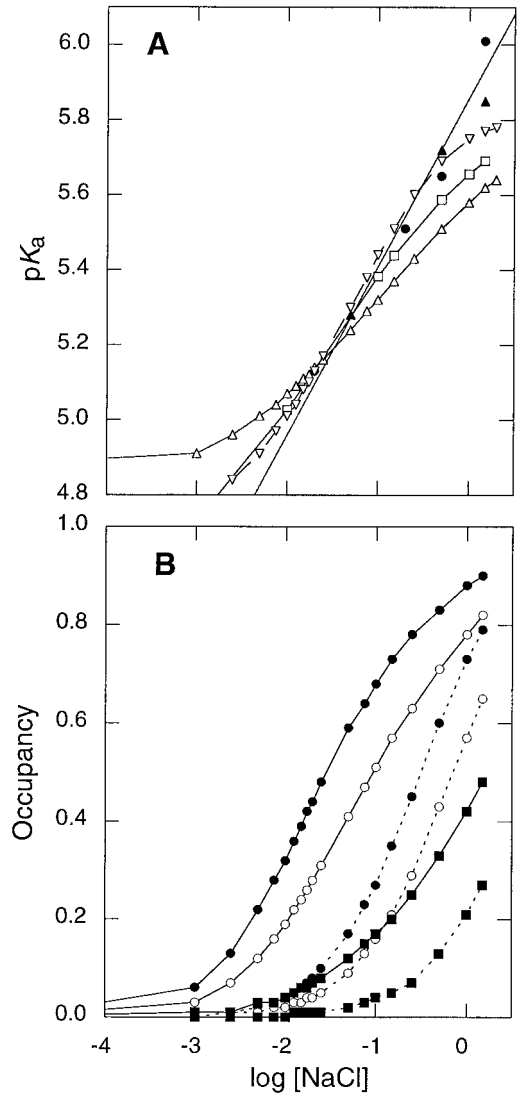

FIGURE 8 (*A*) Comparison between calculated and observed pK_a values of His^{113} in Pc-Mb. A thin solid line represents the linear fit to the experimental values (●). ▲, The pK_a values of His in the FKHLK peptide, shifted along the ordinate to force coincidence with the pK_a of His^{113} at 0.02 M NaCl. Solid lines join the pK_a values calculated with SATK (△) and with FDPB with D_{prot} = 20 (□). pK_a values calculated with FDPB have been shifted to force coincidence with the pK_a of His^{113} at 0.02 M NaCl. ▽, pK_a values calculated with a modification of the SATK algorithms that includes the effects of a chloride ion bound between His^{113} and Arg^{31}. This set of pK_a values has been shifted to force coincidence with the experimental values at 0.02 M NaCl. (*B*) Occupancy of the chloride binding site at pH 7 (——) and pH 4 (·····), calculated with values for K_{int} in Eq. 4 of 1.0 (●), 0.5 (○), and 0.01 (■).

state of His^{113} and the occupancy of the anion binding site were treated explicitly. The possibility of an anion binding event in this region of the protein was predicted by the magnitude of the surface electrostatic potential computed with the empirical Eq. 3 at pH 5. This was one of two regions in the protein where the electrostatic potential calculated with this equation exceeded $+2kT$ (the other region involved Lys^{42} and Lys^{98}).

The explicit consideration of site-specific Cl^- binding improved the agreement between the calculated and the observed salt dependence of the pK_a of His^{113} (Fig. 8 *A*). The data in Fig. 8 *B* show that anion binding at the His^{113}/Arg^{31} site is weak even under conditions of low pH, when the magnitude of the positive electrostatic potential at the site is highest. The binding site was not saturated, even at high salt concentrations. The effects of the site-bound Cl^- on the pK_a of His^{113} were modest but were sufficient to account for the observed behavior.

Salt dependence of Coulombic and self-energy contributions to pK_a values

pK_a values estimated with FDPB calculations include contributions from Coulombic energy (interactions between ionizable groups), Born energy (penalty for removing a charged group from bulk solvent), and background energy (interactions of an ionizable group with partial charges) (Antosiewicz et al., 1994, 1996, and references therein). The salt dependence of the three different energy terms was analyzed separately. Representative data for class 1, 2, and 3 histidines are shown in Fig. 9. The solvation energy calculated with FDPB for the blocked histidine is presented for comparison. Fig. 9 illustrates that in all cases the Born and background energies were nearly insensitive to salt concentration. The net effect of ionic strength on pK_a values mirrors the effect on the charge-charge interactions.

DISCUSSION

The effects of salts on stability and other physical properties of proteins are generally discussed in terms of three different mechanisms: general ionic strength effects, specific salt effects, and effects mediated by water structure alteration. The general ionic strength effect is thought to operate by screening electrostatic interactions between charged groups. Specific salt effects involve direct, chemical interactions between ions and proteins, presumably through the disruption of the primary hydration shells of the ions and their ligands. These effects are usually interpreted as site-specific ion binding when they are observed at low salt concentrations. The remaining indirect effects exert their influence on the properties of water and perturb the interactions between proteins and ions. These types of effects are species specific, and they are most commonly observed at high salt concentrations. The present study offers insight into the nature and relative magnitude of different kinds of contributions to observed salt effects.

A notable feature of the pK_a values measured for class 1 histidines in Mb was the increase they experienced with increased salt concentration. At first glance this would ap-

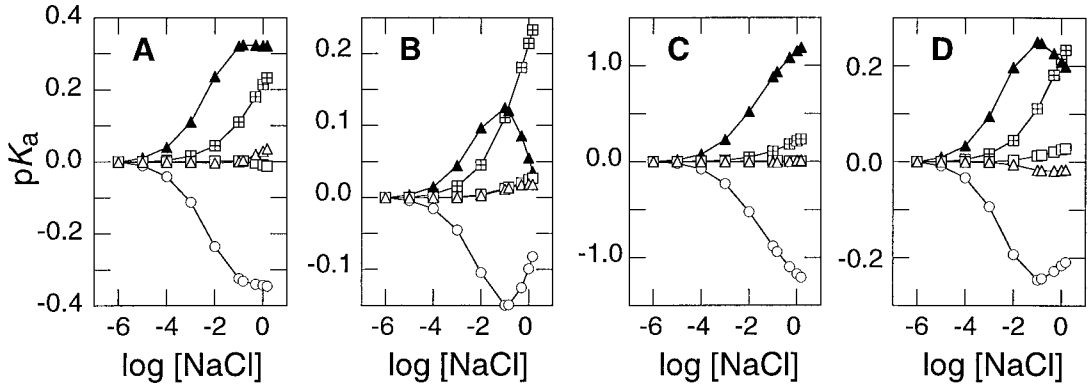

FIGURE 9 Change in calculated pK_a resulting from increasing salt concentration. (*A*) His^{12}. (B) His^{36}. (*C*) His^{113}. (*D*) His^{116}. The total effect obtained by the FDPB method using $D_{prot} = 20$ (▲) is decomposed into Coulombic (○), Born (□), and background (△) energy terms. Note that the vertical scale in each of the panels spans a different range of values. The total salt-induced ΔpK_a estimated from solvation energies of a blocked histidine calculated by FDPB is shown in each panel (⊞) for scaling purposes. In all curves, the value at 1 μM salt concentration was subtracted from each data point to achieve a ΔpK_a at 0 in the limit of low salt concentration.

pear to confirm the notion, rooted in the smeared charge model of Linderstrøm-Lang (1924), that the salt dependence of a pK_a is determined primarily by the difference between it and the pI of the protein. This concept implies that the effects of long-range electrostatic interactions on ionization constants are substantial. In the calculations with the FDPB method, long-range Coulombic interactions contribute significantly to the calculated pK_a values, even when the protein interior is treated with dielectric constants as high as 20. The increase in the pK_a values of class 1 histidines with increasing ionic strength estimated with FDPB calculations (Fig. 6 *B*) reflects the fact that the pI of Mb is greater than 8 (Fig. 5). The net charge of the protein in the range of pH where histidines ionize is positive, and the pK_a values increase when the net repulsive long-range interactions are screened at high salt concentrations.

Interestingly, the pK_a values of histidines in model compounds also increased with increasing salt concentration, and by an amount comparable to that measured for class 1 histidines in Mb (Figs. 3 and 4). This effect was independent of the net charge of the model compound; it was present even in compounds without any charged sites aside from histidine, and in imidazole, which lacks the peptide backbone. Similar salt dependencies have been observed previously. For example, the high concentration of guanidine hydrochloride used in denaturational studies of proteins is known to raise the pK_a of histidines by ~0.2 units (Nozaki and Tanford, 1967), and the pK_a of histidines in human and hen egg white lysozyme increases in the same manner with the addition of salt (Takahashi et al., 1992).

The similarity in the pK_a increases measured in Mb and in model compounds suggests that the response of individual class 1 histidines is not dominated by screening of long-range electrostatic interactions. In agreement with this interpretation, removal of the heme group from Mb, a positively charged moiety buried in the interior, has little effect on the pK_a of most histidines (Cocco et al., 1992). The effects of mutation of ionizable groups on the stability of other proteins are also consistent with the notion that long-range electrostatic interactions in proteins are weaker than predicted by the FDPB algorithm (Dao-pin et al., 1991).

It is possible to explain the observed salt dependence of histidine pK_a values in terms of the effects of counterions on the relative populations of the acidic and the conjugate base form of histidines. The imidazolium ion can interact favorably with the anions in the ion atmosphere hovering about the charged atom and perhaps even form weak complexes (Daniele et al., 1989). Thus at high salt concentrations the charged species would be preferentially populated over the neutral one, resulting in an apparent pK_a increase. This is consistent with the increase in pK_a predicted by FDPB calculations solely on the basis of the ionic strength dependence of the solvation energy of a blocked histidine. Alternatively, the rise in pK_a at higher salt concentrations could be rationalized in terms of the effects of salts on the hydration of ionizable residues. These Hofmeister-type effects cannot be excluded with the data at hand.

In contrast to the behavior of class 1 histidines and histidines in model compounds, the pK_a values of acidic residues in lysozyme (Abe et al., 1995) and in the N-terminal domain of L9 (Kuhlman et al., 1999) and of acidic residues (Schaller and Robertson, 1995) and lysines (Forsyth et al., 1998) in the ovomucoid third domain did not shift in the direction expected if the stabilization of the charged form of an ionizable group through interactions with the counterion cloud were the source of the salt dependence of ionization constants. By this interpretation, the pK_a of carboxylic acids would be expected to decrease with increasing ionic strength. This is in fact observed in fragments of the N-terminal domain of L9, where some, but not

all, of the electrostatic influences that determine the pK_a values are eliminated. However, in folded proteins the pK_a values of acidic residues actually increase, although never to the value measured in model compounds.

Two factors could explain the difference in the effects of salt on the pK_a values of carboxylic groups and histidines. First, carboxylic groups are better hydrated than basic groups (Collins, 1997); complexation with cations might be less effective than complexation between amines and imidazoles and weakly hydrated anions such as Cl^- and Br^-. Second, the ionization equilibria of carboxylic groups are measured at acidic pH. Under these conditions most proteins bear a significant net positive charge, and the attenuation of the net stabilizing long-range electrostatic interactions by the ionic strength would be expected to contribute significantly to the observed salt dependence of pK_a values. This also applies in the titration of lysines at the other end of the pH scale. The difference in the response to salt between lysines and histidines does not appear to derive from intrinsic differences between amines and imidazoles, because the response of the amino terminus of Pc-Mb is indistinguishable from that of histidines (Table 1).

A second noteworthy observation was the salt independence of the pK_a of His^{36}. His^{36} (class 2) has an elevated pK_a thought to reflect the existence of an ion pair with Glu^{38}. The salt-induced changes in pK_a calculated for this residue with the FDPB and SATK methods were in reasonable agreement with the experimental values (Fig. 7). Fig. 9 *B* illustrates that below 0.10 M NaCl the response of His^{36} is determined by the screening of repulsive interactions with other basic groups. At NaCl $>$ 0.10 M, the direction of the pK_a shift changes as the screening of the favorable interactions between His^{36} and Glu^{38} begins to rule the overall behavior. In contrast to the response calculated with structure-based methods, arguments based on simple Debye-Hückel approximations as expressed in Eq. 7 indicate that the pK_a of this ion-paired group should be depressed by a substantial amount at high ionic strength (Fig. 7).

Ion pairs that are insensitive to salt at concentrations of 1.5 M or more have been reported previously (Lyu et al., 1992; Scholtz et al., 1993; Smith and Scholtz, 1998). These experimental observations can be explained if ion pairs behave more like hydrogen bonds than like pairs of point charges interacting through Coulombic forces. However, the FDPB calculations in Fig. 7 and earlier reports (Hendsch and Tidor, 1994) show that ion pairs can be insensitive to ionic strengths as high as 1.5 M, even when they are treated in strictly electrostatic terms. The difference between the behavior of His^{36} calculated with FDBP and the behavior of a histidine in an ideal ion pair in water calculated with Eq. 7 can be explained partly in terms of the screening of long-range repulsive interactions. The distinct behavior also stems from the differences in Coulombic interactions occurring through the protein medium in the case of the ion pair at the surface of the protein, rather than through the aqueous medium, as in the case of the ideal ion pair described by Eq. 7. Counterions cannot penetrate into the protein substance; therefore Coulombic interactions through the protein substance are salt insensitive compared to the interactions happening through solvent.

The low sensitivity of His^{48} to salt concentration can be rationalized in similar terms. The pK_a of this histidine is depressed relative to model compound values for reasons that are not structurally clear. The FDPB calculations showed that both the Coulombic and the Born terms contribute significantly to the depressed pK_a of this histidine. This group adopts the Nϵ2H tautomeric form in the neutral state and has a Nδ1 site with low solvent accessibility (Bhattacharya et al., 1997). If the increase in pK_a values with increasing salt concentration observed for the other Class 1 histidines reflects preferential interactions of the charged form of the imidazole group with the ionic double layer, charged moieties incapable of interacting with anions owing to burial, such as the Nδ1 site of His^{48}, are not expected to display the signature increase in pK_a at high salt concentrations.

The strong ionic interactions between His^{113} and Arg^{31} in Mb constitute a useful model system in which to study the effects of salts on the properties of clusters of basic residues. Clusters of charged groups of the same polarity are rare in proteins. Where found, they usually represent structural adaptations of functional and regulatory significance. Calcium binding sites and the clusters of carboxylates that regulate the self-assembly of some RNA viruses are striking examples of such clusters (Namda and Stubbs, 1986). Clusters of basic residues are rarest (Zhu and Karlin, 1996), and the structural reasons for this are not clear. It might reflect an adaptation to minimize random binding of the abundant intracellular anionic metabolites to the surfaces of proteins. Some proteins have evolved to harness anion binding for regulatory purposes. For example, the clusters of basic residues at the interface between subunits in human hemoglobin are where the functionally significant coupling between heme ligands, protons, chloride ions, and diphosphoglycerate originates. The effects of salts on the stability and ligand binding properties of hemoglobin are usually treated with binding formalisms that imply direct, chemical interactions between anions and clusters of basic residues (García-Moreno, 1994).

His^{113} and the histidine in the FKHLK peptide are the residues that exhibited the most dramatic salt effects. These two histidines have in common the nearby presence of basic groups. (According to the calculations, His^{12} and His^{119} are also in environments with a net positive electrostatic potential. However, in the NMR experiments neither exhibited the depressed pK_a and extreme sensitivity to salt concentration shown by His^{113}, reinforcing the idea that long-range electrostatic interactions are weaker than predicted by FDPB calculations.) The effects of salt concentration on the pK_a of His^{113} were captured relatively well by both SATK

and FDPB calculations, with a slightly better performance by the latter. The best agreement between experimental and calculated behavior was with the set of SATK calculations in which site-specific anion binding to the His^{113}-Arg^{31} pair was treated explicitly. The predicted chloride binding was weak but sufficient to account for the shift in the pK_a of His^{113} up to 1 M NaCl. Interestingly, the predicted Cl^- binding constants calculated with $K_{int} = 1$ M (Eq. 4) are in the same range as those measured experimentally in other systems (Amiconi et al., 1985; Goto et al., 1994). Note that even the anion-binding model did not account for the shift in the pK_a of His^{113} at high anion concentration. The agreement between observed and calculated ionization constants above 1.0 M NaCl could have been improved by using K_{int} other than 1 M, but at the expense of the agreement at the lower salt concentrations.

Weak anion binding is difficult to confirm experimentally. pK_a values measured by ^{1}H-NMR spectroscopy in the presence of 0.2 M KBr (Table 1) were within experimental error of the values measured in NaCl, as expected for two ions with similar solvation enthalpies. Measurements with NaF were performed, but these were limited for three reasons: 1) fluoride ions bind to the ferric heme iron with an association constant of only $\sim 60\ M^{-1}$ (Aime et al., 1996), 2) hydrofluoric acid is a weak acid, and 3) the protein samples in high fluoride concentrations were not as stable as in chloride. Nevertheless, titration curves monitored between pH 6.2 and pH 9.6 for Eq-metMbF in the presence of nearly 1.5 M NaF parallel those obtained in 1.5 M NaCl (data not shown). In theory, the effect of F^- should have been smaller than the effect of Cl^- if the salt dependence of His^{113} were influenced significantly by anion binding and if anion binding involved substantial dehydration of the anion (Collins, 1997). It is difficult to assess what the difference between the effects of these two ions would be if they interacted with the protein without significant disruption of their first solvation layer.

The observed effects of salt on histidine pK_a values have important implications for the interpretation of salt effects on different types of equilibrium processes in proteins. For example, the salt dependence of the first acid denaturational transition of Mb (N to I) has been interpreted previously in terms of the weakening of ion pairs in the native (N) state with increasing ionic strength (Flanagan et al., 1983; Yang and Honig, 1994). The data in Fig. 7 suggest that ion pairs are insensitive to the ionic strength over a wide range of salt concentrations. The data in Figs. 2 and 3 suggest that instead, the shift in the equilibrium between N and I states toward the I state under conditions of increasing salt concentration could arise from the unmasking of neutral, buried histidines in the N state that become charged and solvent exposed in the I state. Favorable interactions between anions and the charged histidines will shift the equilibrium in favor of the I state under conditions of high salt. In general, conformational transitions of a protein where buried histidines become exposed to solvent will exhibit salt dependence, reflecting changes in the solvation of the imidazole group.

The effects of salts on phenomenological equilibrium constants are usually interpreted in terms of "thermodynamically bound" ions (see Makhatadze et al., 1998, for a recent example). The present study suggests that for anion-linked equilibrium processes near neutral pH, the population of thermodynamically bound ions is equivalent to a population of site-bound anions. The salt dependence of the transition between oxy (R) and deoxy (T) of human hemoglobin serves as a representative example. This is an anion-linked process, and the linkage is often treated structurally through preferential anion binding to the T state (Amiconi et al., 1981). In this case the measured salt dependence reflects the difference in the interactions between ions and the two different quaternary states of the protein. Near neutral pH the number of solvent-exposed basic residues is the same in the two quaternary states. The similarity in the salt dependence of pK_a values of histidines in model compounds and Mb suggests that solvent-exposed histidines will not contribute significantly to the salt dependence of the equilibrium between the R and T states. The data in Fig. 7 show that the stability of ion pairs can be independent of salt concentration. Therefore, the dominant source of salt dependence in the R-to-T transition must involve the effects of salt on the repulsive interactions in clusters of basic groups, similar to what was observed for His^{113} in Pc-Mb.

The reason for comparing observed and calculated pK_a values was to assess the ability of continuum methods to capture the dependence of ionization equilibria on salt concentration. These methods are based on the linearized Poisson-Boltzmann equation, which is formally not valid at most of the ionic strengths where pK_a values were measured. However, the ionic strengths of physiological interest are themselves beyond the theoretical limit of validity. For this reason, structure-based pK_a calculations are usually performed at salt concentrations above the upper limit, and it is of interest to determine the capabilities of the methods under these conditions. The experimental data (Figs. 2–4) suggested that the FDPB method failed to reproduce important aspects of the salt dependence of histidine pK_a values, especially at salt concentrations above 0.1 M. For His^{48} and His^{81}, which are isolated and without nearby ionizable groups, FDPB calculations succeeded in simulating the experimental increase in pK_a with increasing salt concentration. However, for the remaining class 1 histidines (12, 116, and 119) the calculated and the experimental behavior began to diverge at low salt concentrations.

This study underscores two general problems with the FDPB calculations. First, the magnitude of electrostatic interactions between surface residues is exaggerated in calculations with static structures, even when the interior of the protein is treated with arbitrarily high dielectric constants. Consequently, screening of electrostatic interactions by the

ionic strength is also exaggerated. Second, the pK_a values of model compounds are sensitive to salt, and this is never considered explicitly in pK_a calculations.

The solvation energy of a blocked histidine calculated with the FDPB method reproduced the salt dependence of model compound pK_a values well. This suggests that the ability of the FDPB method to estimate the salt dependence of pK_a values can be improved by including the solvation energy term explicitly. A correction to account for the ionic strength effect on the reference pK_a would shift the calculated pK_a values by equivalent amounts along the ordinate. The data in Figs. 6–8 imply that these corrections would improve the agreement between the observed and measured salt dependence of pK_a values in some cases and worsen it in others. Furthermore, it is not obvious that this correction will improve the agreement between observed and calculated behavior at the highest salt concentrations that were studied. Further improvement will depend on the ability to estimate more realistic Coulombic energies (interactions between ionizable groups). The explicit treatment of conformational flexibility is one strategy that seems to improve the agreement between calculated and observed pK_a values (Havranek and Harbury, 1999, and references therein). In electrolyte solutions the efficiency with which a charge can be screened was found to depend markedly on the frequency of its oscillations (Vallejo and Grigera, 1994). This suggests that rigorous treatment of the dynamics of ionizable groups in turn will yield more realistic estimates of the salt dependence of electrostatic interactions in proteins.

The finding that FDPB calculations overestimate the magnitude of long-range electrostatic interactions does not imply that long-range effects are not significant and that screening of these electrostatic interactions is not an important factor influencing the stability of proteins. For example, under acidic conditions where the net positive charge of most proteins is high, screening effects can be substantial (Goto et al., 1990). It is also likely that in proteins with a higher isoionic point than Mb the difference in pK_a values of histidines in low and high salt concentrations will be greater than what was observed for the histidines in Mb. In those cases the contributions by screening of long-range electrostatic interactions by the ionic strength would be expected to contribute more significantly to the salt dependence of pK_a values.

The experimental data in this study emphasize the need to revisit some notions frequently invoked in the structural interpretation of the salt dependence of protein energetics. Specifically, the salt dependence of histidine pK_a values is not always related to the isoionic point of the protein. The data suggest that medium- and long-range electrostatic interactions in proteins are weaker than previously recognized and that structure-based calculations with the FDPB method, using static structures, exaggerate the magnitude of electrostatic effects, even when the protein interior is treated as a medium with high dielectric constant. Screening of Coulombic interactions between ionizable groups is not the dominant source of salt dependence of histidine pK_a values in Mb. Even the energy of interaction between strongly ion-paired groups appears to be insensitive to salt at concentrations as high as 1.5 M. Only in the case of histidines with significant net destabilizing interactions with other basic groups was the salt dependence of the pK_a strongly influenced by screening, and in those cases site-specific anion binding can be invoked to improve the estimated salt dependence of a pK_a.

The authors thank Dr. John Dwyer for measurement of the potentiometric proton titration curves, Ms. Joyce Lilly for peptide synthesis, and Prof. A. McCammon and Dr. M. Gilson for providing the UHBD software suite and patient instruction on its application for pK_a calculations. The authors also thank Nancy Scott for assistance in preparing metfluoromyoglobin samples.

This work was supported by grant GM-54217 (formerly DK-43101) from the National Institutes of Health (JTJL) and by grant MCB-9600991 from the National Science Foundation (BGME).

REFERENCES

Abe, Y., T. Ueda, H. Iwashita, Y. Hashimoto, H. Motoshima, Y. Tanaka, and T. Imoto. 1995. Effect of salt concentration on the pK_a of acidic residues in lysozyme. *J. Biochem.* 118:946–952.

Aime, S., M. Fasano, S. Paoletti, F. Cutruzzola, A. Desideri, M. Bolognesi, M. Rizzi, and P. Ascenzi. 1996. Structural determinants of fluoride and formate binding to hemoglobin and myoglobin: crystallographic and ^{1}H-NMR relaxometric study. *Biophys. J.* 70:482–488.

Amiconi, G., E. Antonini, M. Brunori, J. Wyman, and L. Zolla. 1981. Interaction of hemoglobin with salts. *J. Mol. Biol.* 152:111–129.

Antosiewicz, J., J. A. McCammon, and M. K. Gilson. 1994. Prediction of pH-dependent properties of proteins. *J. Mol. Biol.* 238:415–436.

Antosiewicz, J., J. A. McCammon, and M. K. Gilson. 1996. The determinants of pK_a's in proteins. *Biochemistry.* 35:7819–7833.

Barrick, D., F. M. Hughson, and R. L. Baldwin. 1994. Molecular mechanisms of acid denaturation. The role of histidine residues in the partial unfolding of apomyoglobin. *J. Mol. Biol.* 237:588–601.

Bashford, D., D. A. Case, C. Dalvit, L. Tennant, and P. E. Wright. 1993. Electrostatic calculations of side-chain pK_a values in myoglobin and comparison with NMR data for histidines. *Biochemistry.* 32:8045–8056.

Bhattacharya, S., and J. T. J. Lecomte. 1997. Temperature dependence of histidine ionization constants in myoglobin. *Biophys. J.* 73:3241–3256.

Bhattacharya, S., S. F. Sukits, K. L. MacLaughlin, and J. T. J. Lecomte. 1997. The tautomeric state of histidines in myoglobin. *Biophys. J.* 73:3230–3240.

Bothner-By, A. A., R. L. Stephens, J.-M. Lee, C. D. Warren, and R. W. Jeanloz. 1984. Structure determination of a tetrasaccharide: transient nuclear Overhauser effects in the rotating frame. *J. Am. Chem. Soc.* 106:811–813.

Braunschweiler, L., and R. R. Ernst. 1983. Coherence transfer by isotropic mixing: application to proton correlation spectroscopy. *J. Magn. Reson.* 53:521–528.

Brunori, M., G. Amiconi, E. Antonini, J. Wyman, R. Zito, and R. Fanelli. 1968. The transition between "acid" and "alkaline" ferric heme proteins. *Biochim. Biophys. Acta.* 154:315–322.

Cavanagh, J., and M. Rance. 1992. Suppression of cross-relaxation effects in TOCSY spectra via a modified DIPSI-2 mixing sequence. *J. Magn. Reson.* 96:670–678.

Chu, A., B. W. Turner, and G. K. Ackers. 1984. Effects of protons on the oxygenation-linked subunit assembly in human hemoglobin. *Biochemistry.* 23:604–617.

Cocco, M. J., Y.-H. Kao, A. T. Phillips, and J. T. J. Lecomte. 1992. Structural comparison of apomyoglobin and metaquomyoglobin: pH titration of histidines by NMR spectroscopy. *Biochemistry*. 31: 6481–6491.

Collins, K. D. 1997. Charge density-dependent strength of hydration and biological structure. *Biophys. J.* 72:65–76.

Dang, Q. D., and E. Di Cera. 1996. Residue 225 determines the Na^+-induced allosteric regulation of catalytic activity in serine proteases. *Proc. Natl. Acad. Sci. USA.* 93:10653–10656.

Daniele, P. G., A. De Robertis, C. De Stefano, and S. Sammartano. 1989. Salt effects on the protonation of imidazole in aqueous solution at different ionic strengths. A tentative explanation by a complex formation model. *J. Sol. Chem.* 18:23–36.

Dao-pin, S., E. Soderlind, W. A. Baase, J. A. Wozniak, U. Sauer, and B. W. Matthews. 1991. Cumulative site-directed charge-charge replacements in T4 lysozyme suggest that long-range electrostatic interactions contribute little to protein stability. *J. Mol. Biol.* 221:873–887.

Davies, C. W. 1938. The extent of dissociation of salts in water. Part VIII. An equation for the mean ionic activity coefficient of an electrolyte in water, and a revision of the dissociation constants of some sulphates. *J. Chem. Soc.* 2093–2098.

Davies, M. E., J. D. Madura, B. A. Luty, and J. A. McCammon. 1991. Electrostatics and diffusion of molecules in solution—simulations with the University of Houston Brownian Dynamics program. *Comput. Phys. Commun.* 62:87–197.

Elcock, A. H., and J. A. McCammon. 1998. Electrostatic contributions to the stability of halophilic proteins. *J. Mol. Biol.* 280:731–748.

Flanagan, M. A., B. García-Moreno, S. H. Friend, R. J. Feldmann, H. Scouloudi, and F. R. Gurd. 1983. Contributions of individual amino acid residues to the structural stability of cetacean myoglobins. *Biochemistry.* 22:6027–6037.

Forsyth, W. R., M. K. Gilson, J. Antosiewicz, O. R. Jaren, and A. D. Robertson. 1998. Theoretical and experimental analysis of ionization equilibria in ovomucoid third domain. *Biochemistry.* 37:8643–8652.

Fox, J. M., X. Zhao, J. A. Speir, and M. J. Young. 1996. Analysis of a salt stable mutant of cowpea chlorotic mottle virus. *Virology.* 222:115–122.

García-Moreno, E. B. 1994. Estimating binding constants for site-specific interactions between monovalent ions and proteins. *Methods Enzymol.* 240:645–667.

García-Moreno, E. B., L. X. Chen, K. L. March, R. S. Gurd, and F. R. N. Gurd. 1985. Electrostatic interactions in sperm whale myoglobin. *J. Biol. Chem.* 260:14070–14082.

García-Moreno, E. B., J. J. Dwyer, A. G. Gittis, E. E. Lattman, D. S. Spencer, and W. E. Stites. 1997. Experimental measurement of the effective dielectric in the hydrophobic core of a protein. *Biophys. Chem.* 64:211–224.

Gilson, M. K. 1993. Multi-site titration and molecular modeling: two rapid methods for computing energies and forces for ionizable groups in proteins. *Proteins Struct. Funct. Genet.* 15:266–282.

Goto, Y., L. J. Calciano, and A. L. Fink. 1990. Acid-induced folding of proteins. *Proc. Natl. Acad. Sci. USA.* 7:573–577.

Havranek, J. J., and P. B. Harbury. 1999. Tanford-Kirkwood electrostatics for protein modeling. *Proc. Natl. Acad. Sci. USA.* 96:11145–11150.

Hendsch, Z. S., and B. Tidor. 1994. Do salt bridges stabilize proteins? A continuum electrostatic analysis. *Protein Sci.* 3:211–226.

Hochmann, J., and H. J. Kellerhals. 1980. Proton NMR on deoxyhemoglobin. Use of a modified DEFT technique. *J. Magn. Reson.* 38:23–39.

Inubushi, T., and E. D. Becker. 1983. Efficient detection of paramagnetically shifted NMR resonances by optimizing the WEFT pulse sequence. *J. Magn. Reson.* 51:128–133.

Jencks, W. P. 1987. Catalysis in Chemistry and Enzymology. Dover Publications, New York. 351–392.

Jorgensen, W. L., and J. Tirado-Rives. 1988. The OPLS potential functions for protein energy minimization for crystals of cyclic peptides and crambin. *J. Am. Chem. Soc.* 110:1657–1666.

Kao, Y.-H. 1994. A study of metaquomyoglobin in solution by NMR spectroscopy. Structural properties and histidine ionization. Ph.D. thesis. The Pennsylvania State University, University Park, PA.

Kao, Y.-H., and J. T. J. Lecomte. 1993. Determination of the zero-field splitting constant for proton NMR chemical shift analysis in metaquomyoglobin. The dipolar shift as a structural probe. *J. Am. Chem. Soc.* 115:9754–9762.

Klapper, I., R. Hagstrom, R. Fine, K. Sharp, and B. Honig. 1986. Focusing of electric fields in the active site of Cu-Zn superoxide dismutase: effects of ionic strength and amino-acid modification. *Proteins Struct. Funct. Genet.* 1:47–59.

Kozlov, A. G., and T. M. Lohman. 1998. Calorimetric studies of *E. coli* SSB protein-single-stranded DNA interactions. Effects of monovalent salts on binding enthalpy. *J. Mol. Biol.* 278:999–1014.

Krishnamoorthy, R., and G. N. La Mar. 1984. Identification of the titrating group in the heme cavity of myoglobin. Evidence for the heme-protein pi-pi interaction. *Eur. J. Biochem.* 138:135–140.

Kuhlman, B., D. L. Luisi, P. Young, and D. P. Raleigh. 1999. pK_a values and the pH dependent stability of the N-terminal domain of L9 as probes of electrostatic interactions in the denatured state. Differentiation between local and nonlocal interactions. *Biochemistry.* 38:4896–4903.

Kumar, A., R. R. Ernst, and K. Wüthrich. 1980. A 2D NOE experiment for the elucidation of complete proton-proton cross-relaxation networks in biological macromolecules. *Biochem. Biophys. Res. Commun.* 95:1–6.

La Mar, G. N., J. D. Satterlee, and J. S. de Ropp. 2000. Nuclear magnetic resonance of hemoproteins. *In* The Porphyrin Handbook. K. M. Smith, K. Kadish, and R. Guilard, editors. Academic Press, Burlington, MA. 185–298.

Linderstrøm-Lang, K. 1924. On the ionization of proteins. *C. R. Trav. Lab. Carlsberg.* 15:1–29.

Lyu, P. C., P. J. Gans, and N. R. Kallenbach. 1992. Energetic contribution of solvent-exposed ion pairs to alpha-helix structure. *J. Mol. Biol.* 223:343–350.

Makhatadze, G. I., M. M. Lopez, J. M. Richardson, and S. T. Thomas. 1998. Anion binding to the ubiquitin molecule. *Protein Sci.* 7:689–697.

Markley, J. 1975. Observation of histidine residues in proteins by means of nuclear magnetic resonance spectroscopy. *Acc. Chem. Res.* 8:70–80.

Matthew, J. B., F. R. N. Gurd, B. García-Moreno E., M. A. Flanagan, K. L. March, and S. J. Shire. 1985. pH dependent processes in proteins. *CRC Crit. Rev. Biochem.* 18:91–197.

Namda, K., and G. Stubbs. 1986. Structure of tobacco mosaic virus at 3.6 Å resolution: implications for assembly. *Science.* 231:1401–1406.

Nozaki, Y., and C. Tanford. 1967. Acid-base titrations in concentrated guanidine hydrochloride. Dissociation constants of the guanidinium ion and of some amino acids. *J. Am. Chem. Soc.* 89:736–742.

O'Brien, R., B. DeDecker, K. G. Fleming, P. B. Sigler, and J. E. Ladbury. 1998. The effects of salt on the TATA binding protein-DNA interaction from a hyperthermophilic archaeon. *J. Mol. Biol.* 279:117–125.

Pace, C. N., and G. R. Grimsley. 1988. Ribonuclease T is stabilized by cation and anion binding. *Biochemistry.* 27:3242–3246.

Pieper, U., G. Kapadia, M. Mevarech, and O. Herzberg. 1997. Structural features of halophilicity derived from the crystal structure of dihydrofolate reductase from the Dead Sea halophilic archaeon *Haloferz volcanii. Structure.* 6:75–88.

Piotto, M., V. Saudek, and V. Sklenár. 1992. Gradient-tailored excitation for single-quantum NMR spectroscopy of aqueous solutions. *J. Biomol. NMR.* 2:661–665.

Rance, M., O. W. Sørensen, G. Bodenhausen, G. Wagner, R. R. Ernst, and K. Wüthrich. 1983. Improved spectral resolution in COSY ^{1}H NMR spectra of proteins via double quantum filtering. *Biochem. Biophys. Res. Commun.* 117:479–485.

Schaller, W., and A. D. Robertson. 1995. pH, ionic strength, and temperature dependencies of ionization equilibria for the carboxyl groups in turkey ovomucoid third domain. *Biochemistry.* 34:4714–4723.

Scholtz, J. M., H. Qian, V. H. Robbins, and R. L. Baldwin. 1993. The energetics of ion-pair and hydrogen-bonding interactions in a helical peptide. *Biochemistry.* 32:9668–9676.

Scouloudi, H., and E. N. Baker. 1978. X-ray crystallographic studies of seal myoglobin. The molecule at 2.5 Å resolution. *J. Mol. Biol.* 126: 637–660.

Shaka, A. J., C. Lee, and A. Pines. 1988. Iterative schemes for bilinear operators; application to spin decoupling. *J. Magn. Reson.* 77:274–293.

Sklenár, V., M. Piotto, R. Lepik, and V. Saudek. 1993. Gradient-tailored water suppression for ^{1}H-^{15}N HSQC experiments optimized to retain full sensitivity. *J. Magn. Reson.* 102:241–245.

Smith, J. S., and J. M. Scholtz. 1998. Energetics of polar side-chain interactions in helical peptides: salt effects on ion pairs and hydrogen bonds. *Biochemistry.* 37:33–40.

Sudmeier, J. L., J. L. Evelhoch, and N. B.-H. Jonsson. 1980. Dependence of NMR lineshape analysis upon chemical rates and mechanisms: implications for enzyme histidine titrations. *J. Magn. Reson.* 40:377–390.

Takahashi, T., H. Nakamura, and A. Wada. 1992. Electrostatic forces in two lysozymes: calculations and measurements of histidine pK_a values. *Biopolymers.* 32:897–909.

Tanford, C. 1961. Physical Chemistry of Macromolecules. John Wiley and Sons, New York. 548–586.

Vallejo, D. F., and J. R. Grigera. 1994. Frequency effect on the charge screening in electrolyte solutions. Charge fluctuation and spatial oscillations studied by Brownian dynamics simulations. *J. Chem. Phys.* 101:9049–9053.

Warshel, A., S. T. Russell, and A. K. Churg. 1984. Macroscopic models for studies of electrostatic interactions in proteins: limitations and applicability. *Proc. Natl. Acad. Sci. USA.* 81:4785–4789.

Wishart, D. S., C. G. Bigam, J. Yao, F. Abildgaard, H. J. Dyson, E. Oldfield, J. L. Markley, and B. D. Sykes. 1995. ^{1}H, ^{13}C and ^{15}N chemical shift referencing in biomolecular NMR. *J. Biomol. NMR.* 6:135–140.

Wyman, J., and S. J. Gill. 1990. Binding and Linkage. University Science Books, Hill Valley, CA.

Yang, A., and B. Honig. 1994. Structural origins of pH and ionic strength effects of protein stability. *J. Mol. Biol.* 150:602–614.

Zhu, Z. Y., and S. Karlin. 1996. Clusters of charged residues in protein three-dimensional structures. *Proc. Natl. Acad. Sci. USA.* 93: 8350–8355.